

Machine learning versus manual earthquake location workflow: testing LOC-FLOW on an unusually productive microseismic sequence in northeastern Italy

Monica Sugan, Laura Peruzza, Maria Adelaide Romano, Mariangela Guidarelli, Luca Moratto, Denis Sandron, Milton Percy Plasencia Linares & Marco Romanelli

To cite this article: Monica Sugan, Laura Peruzza, Maria Adelaide Romano, Mariangela Guidarelli, Luca Moratto, Denis Sandron, Milton Percy Plasencia Linares & Marco Romanelli (2023) Machine learning versus manual earthquake location workflow: testing LOC-FLOW on an unusually productive microseismic sequence in northeastern Italy, *Geomatics, Natural Hazards and Risk*, 14:1, 2284120, DOI: [10.1080/19475705.2023.2284120](https://doi.org/10.1080/19475705.2023.2284120)

To link to this article: <https://doi.org/10.1080/19475705.2023.2284120>



© 2023 The Author(s). Published by Informa UK Limited, trading as Taylor & Francis Group.



Published online: 23 Nov 2023.



[Submit your article to this journal](#)



Article views: 331











[View related articles](#)



[View Crossmark data](#)

Machine learning versus manual earthquake location workflow: testing LOC-FLOW on an unusually productive microseismic sequence in northeastern Italy

Monica Sugan , Laura Peruzza , Maria Adelaide Romano , Mariangela Guidarelli , Luca Moratto , Denis Sandron , Milton Percy Plasencia Linares  and Marco Romanelli 

National Institute of Oceanography and Applied Geophysics - OGS, Italy

ABSTRACT

It is an open question whether machine-learning (ML) methods can be trusted in areas where dense and localized seismic networks are in operation, and prompt and accurate detection and location of earthquakes are essential to guide decision-making processes that contribute to seismic-risk-mitigation-strategies, even for very low-magnitude events. To address these concerns, we compare the performance of a widely-used ML phase picker, PhaseNet, integrated with several popular earthquake location methods (included in LOC-FLOW), with the results obtained by the workflow adopted since 2012 by the Collalto Seismic Network, installed to monitor natural and potentially induced microearthquakes nearby an underground gas storage. The tested dataset concerns the most populated microseismic sequence observed so far (374 events, $M_L \leq 2.5$, August 2021, Refrontolo, NE-Italy), as its unusual productivity raised some criticalities in the combination of automatic routines, and time-consuming manual revision of phase picks adopted by the standard workflow. LOC-FLOW is able to detect the majority of the events listed in the manually revised catalog, demonstrating its ability to efficiently and accurately build earthquake catalogs from continuous seismic data. We highlight both the advantages and limitations of the ML-picker and recommend the use of template-matching-techniques in the final stage of processing to increase the number of events.

ARTICLE HISTORY


Received 9 June 2023
Accepted 12 November 2023

KEYWORDS

Machine learning; microseismicity; template matching; seismic monitoring; Collalto Seismic Network

1. Introduction

Earthquake detection and seismic phase picking are the basis of many seismological workflows, which are indispensable tools both for seismic monitoring, and detailed seismological studies. Recently, machine-learning (ML) techniques have been widely applied in earthquake location problems (Kong et al. 2019). In particular, ML-based

CONTACT Monica Sugan  msugan@ogs.it

This article has been corrected with minor changes. These changes do not impact the academic content of the article.

© 2023 The Author(s). Published by Informa UK Limited, trading as Taylor & Francis Group.

This is an Open Access article distributed under the terms of the Creative Commons Attribution-NonCommercial License (<http://creativecommons.org/licenses/by-nc/4.0/>), which permits unrestricted non-commercial use, distribution, and reproduction in any medium, provided the original work is properly cited. The terms on which this article has been published allow the posting of the Accepted Manuscript in a repository by the author(s) or with their consent.

automatic picking algorithms have shown great potential to significantly speed up the process of seismic phase picking while maintaining high accuracy (e.g. Ross et al. 2018; Zhu and Beroza 2018; Mousavi et al. 2019; Soto and Schurr 2021). The computational speed of ML algorithms makes them prime candidates also for seismic monitoring and real-time applications. The reliability and stability of machine learning outputs rely on several factors, such as the quality of the data used to train the model, the hyperparameters employed during training, the complexity of the model architecture, and the amount of data used for validation and testing purposes.

In general, it has been demonstrated that ML trained models can be transferred between regions with only slight performance degradation, as long as the investigation distance ranges stay similar (Münchmeyer et al. 2022). So far, ML models have been trained on massive local, regional and teleseismic data, while for very local dense networks there are few specific datasets suitable for training ML algorithms, as their data are limited due to the short operational time of the network, or for the low number of detected earthquakes.

Usually, ML applications in microseismic monitoring are similar to those for earthquake monitoring, but deal with weak seismic signals characterized by low signal-to-noise ratio on individual receivers, or very short target time signals (Anikiev et al. 2023 and references therein).

Thus, testing the performance of ML models trained on regional datasets on a microseismic sequence could be challenging, but very useful as ML could be crucial for seismic monitoring in the field of induced seismicity (e.g. Mousavi et al. 2016) or for near fault observatory activities (Panebianco et al. 2023; Scotto di Uccio et al. 2023). Besides, ML also applied in the post-processing could help in understanding the mechanism of the natural and induced seismicity, as well.

In this study, we evaluate the performance, in terms of phase picks accuracy, event association, and final earthquake origin time and locations, of the PhaseNet algorithm (Zhu and Beroza 2018) trained on California Earthquake Data and considered one of the top deep learning models for earthquake phase identification (see Münchmeyer et al. 2022), as a component of the comprehensive LOC-FLOW earthquake location workflow (Zhang et al. 2022) on the so-called Refrontolo seismic sequence (Peruzza et al. 2022a). This sequence was highly concentrated in space and time, and occurred on an antithetic fault segment of the Montello thrust system in the Pedemontana district in the Southeastern Alps (Sugan and Peruzza 2011) beneath the village of Refrontolo (located between Pieve di Soligo and Conegliano, in northeastern Italy, Figure 1a), in August 2021. It was an exceptionally productive but low energy sequence ($M_L 2.5$ for the main event), with 374 events occurring at about 9 km depth in a very small volume. It is the most populated sequence recorded in the last decade by the permanent Collalto Seismic Network (RSC), made available as a valuable case for testing and refining automated microearthquake ML detection and location procedures (Peruzza et al. 2022b).

The RSC is a local network that thickens the regional one (Sistema di Monitoraggio terrestre dell'Italia Nord Orientale - SMINO; Bragato et al. 2011, 2021), and it is composed of 10 stations (Priolo et al. 2015a) used for monitoring the microseismicity potentially induced by an underground gas storage since 2012. The

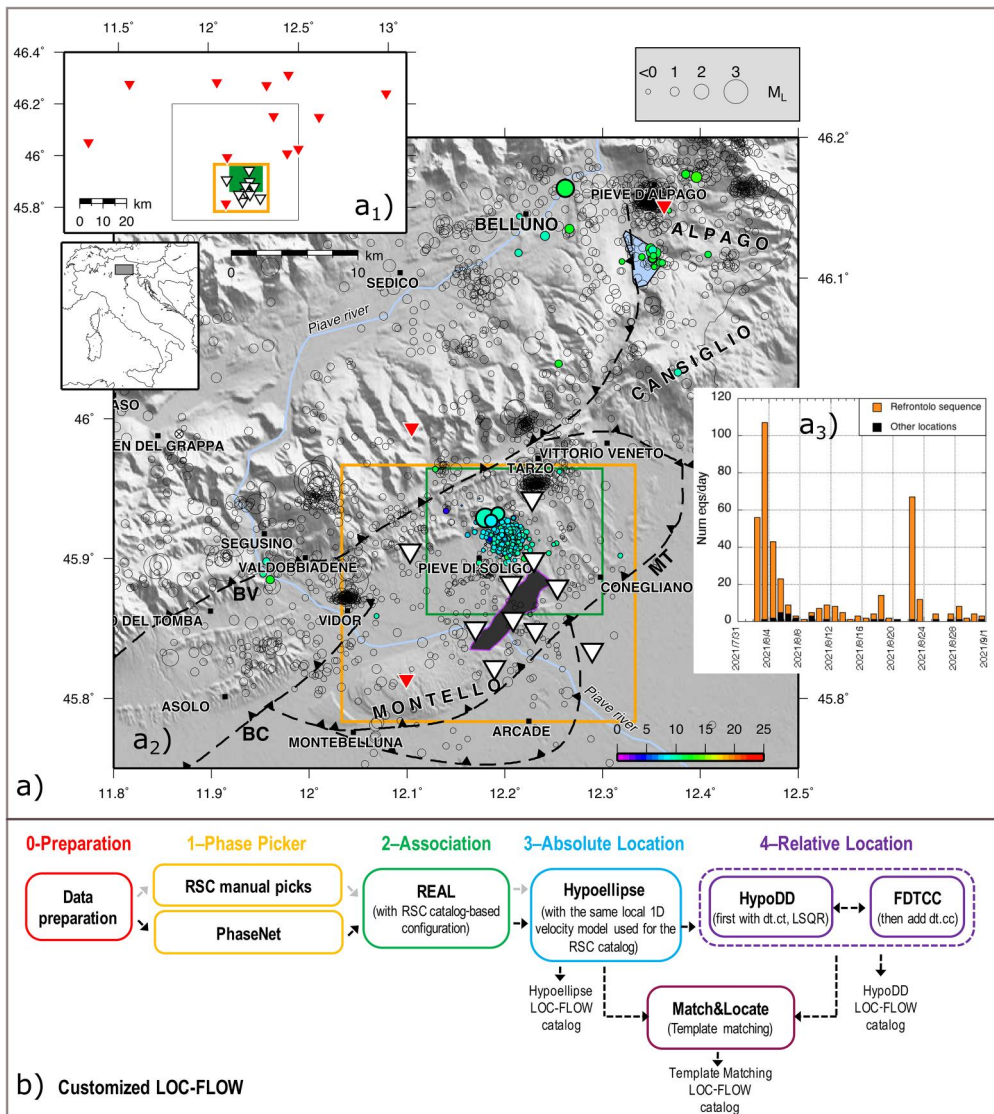


Figure 1. Tested dataset and logic flow of this study. a) Location map of the earthquakes occurred in August 2021 in northern Italy (inset) as given in Peruzza et al. (2022b); a₁) map of the stations used in this work, red triangles belong to the SMINO network (Bragato et al. 2021), white ones to the local Collalto Seismic Network (RSC, Priolo et al. 2015a), color frames indicate respectively the plot area represented in a₂ (black), the target area of the RSC (orange) and the Refrontolo area (near Pieve di Soligo) involved by the unusually productive sequence analyzed (green); a₂) epicentral map with main tectonic element taken from Burrato et al. (2008); MT indicates the Montello thrust; the epicenters symbol size is proportional to local magnitude M_L , depth is color-coded according to scale bar (bottom right) for the events occurred in August, transparent circles show the location of the seismicity detected from 2012 in the region; the black area with purple contour shows the surface projection of the Collalto underground gas storage (UGS); a₃) histogram of the daily number of events manually located by the RSC network in August 2021, referred to the Refrontolo sequence (orange) or to other locations. b) LOC-FLOW processing configuration used in this study (modified from Zhang et al. 2022).

network is managed by the National Institute of Oceanography and Applied Geophysics - OGS on behalf of Edison Stocaggio S.p.A., and provides uniform catalog completeness, and a valuable dataset of observations over more than 11 years. To date, no earthquakes have been associated with methane storage activities; conversely, natural microseismicity has yielded exceptional 3D imaging of the Montello thrust (Moratto et al. 2019; Romano et al. 2019; Picotti et al. 2022), a resource not available when Galadini et al. (2005) hypothesized the existence of a single fault segment capable of M 6.7 earthquakes with an average recurrence interval of about 700 years.

RSC real-time seismic monitoring is performed with a customized workflow of the BRTT Antelope routines (Garbin and Priolo 2013; Moratto and Sandron 2015; Priolo et al. 2015a): automatic earthquake detection is based on STA/LTA algorithms, grid-search location uses the IASPEI global velocity models and multiscale sized grids to discriminate local, regional and teleseismic events, and local magnitude is estimated. Alert conditions are set to activate an immediate manual refinement of location and magnitude estimation by the seismologist on-call. These alerted events represent a small percentage of the final catalog content, because besides the real-time monitoring, a semi-automatic off-line processing takes place daily. It includes: i) recovery of data missing in real-time, ii) manual revision of all possible events detected by Antelope reprocessing new data, and selection of local earthquakes, iii) manual picking and absolute location of local earthquakes only, using standard procedures (e.g. Hypoellipse, Lahr 1999), iv) re-estimation of local magnitude. As data can sometimes be available only several days later, a similar reprocessing is also performed monthly, to obtain the final catalog.

This process of manual control of local events and P and S picking revision, ensures accurate data and associated metadata, lowers the completeness local magnitude to $M_L \sim 0$ in the RSC target area (orange frame in Figure 1a), but it is time-consuming, and may face difficulties during highly-populated seismic sequences that have to be analyzed in a very short time, as happened during the Refrontolo sequence.

Comparing seismic catalogs obtained by associations approved by experienced analysts and revised manual picks with those derived by applying PhaseNet integrated into a high precision earthquake location workflow (LOC-FLOW, Zhang et al. 2022) is therefore a unique opportunity to test the performance of ML methods in earthquake detection and location for local microearthquakes. Concerning automatic phase detection, PhaseNet is trained on a dataset provided by analyst-labeled P and S arrival times from the Northern California Earthquake Data Center Catalog (NCEDC 2014).

Implementing a machine learning-based workflow for high-precision earthquake location can be strategic in supporting RSC seismic monitoring during seismic crises, and could be considered of interest for both the cases of natural and potentially induced seismicity. The utilization of a semi-automated workflow (e.g. Panebianco et al. 2023) has demonstrated great promise in the field of microseismic detection, serving as a crucial starting point towards the subsequent realization of a fully automated system.

In our study, we test PhaseNet capacity to detect microseismicity in the Collalto region, as part of LOC-FLOW. We are particularly interested in: 1) the performances

of PhaseNet's phase picker, compared with the RSC's manual phase picks; 2) the LOC-FLOW-generated earthquake catalogs (origin time and absolute locations) using PhaseNet picks or the original manual RSC's picks; 3) the contribution of template matching to the final LOC-FLOW catalog, versus the original RSC dataset. Magnitudes in the catalogs are beyond the purposes of this analysis.

We also evaluate the spatio-temporal characteristic of the obtained seismicity, evaluating the ability of the customized procedure to identify the tectonic structures activated during the sequence.

2. Method and results

The original LOC-FLOW workflow incorporates open-source packages for seismic data preparation (namely, Step 0), picking strategies (Step 1), phase association (Step 2), as well as absolute (Step 3) and relative double-difference location (Step 4), together with template matching methods. The workflow consists of sequential modules that are cross-compatible in terms of input/output, making them flexible for customized applications. The structure of the code enables users to easily modify the workflow by testing and incorporating different packages across various modules; the formats of the different steps remain compatible to maintain the workflow's functionality. In our study, we adapt the original version (Zhang et al. 2022) to reproduce as faithfully as possible the processing done for obtaining the manual Refrontolo seismic sequence catalog (see Figure 1b): for the '1-Phase picker' module, we used two different configurations, the original P and S picks listed in the RSC catalog characterized by a phase pick weight code [0-3], and the P and S PhaseNet picks characterized by phase pick probabilities [0-1]; for the '3-Absolute location' section, we implement and use the Hypoellipse code (Lahr 1999), running with an existing velocity model optimized for the area monitored by RSC. Hypoellipse was chosen because it was used to locate the events in the reference dataset (Peruzza et al. 2022b). We calibrate the ML picking probability estimate provided by PhaseNet with the P- and S-phase weight code obtained by manual revision, based on the picking uncertainty.

To prepare the data and estimate the performances of LOC-FLOW, we proceed as follows.

First, we collect continuous seismic waveforms from August 2 to 31 for stations located at a maximum distance of 50 km from the Refrontolo sequence (0-Preparation); this waveform dataset includes 22 stations (all the RSC stations plus another 12 belonging to the SMINO Network), shown in Figure 1a₁. The seismic waveforms are resampled homogeneously at 100 Hz.

At LOC-FLOW Step 1, initially we use the original manually revised P and S picks reported in the RSC catalog for the analyzed time period (August 2021), to tune and test the performance of the associator (Step 2). We consider this step necessary to properly compare these results with the one achievable using the ML picker directly in the LOC-FLOW procedure. During the analyzed time span, the RSC catalog contains about 3519 and 2884 picks for P and S seismic phases respectively, for a total of 407 local events, of which 374 are related to the Refrontolo seismic sequence (green frame in Figure 1a, the target area of RSC represented by the orange frame). The

other locations (see [Figure 1a₃](#)) are part of a small cluster that occurred in the Belluno-Alpago area (located about 30 km northeast of Refrontolo, with a maximum local magnitude of 2.3, near Pieve D'Alpago), and a few ones occurred near Valdobbiadene (about 20 km westwards). We include all the available picks in our evaluation to assess the performance of LOC-FLOW also at the border of the best-monitored region. The RSC picks also include 7 additional stations more than 50 km away, for which very few picks were reported for the most energetic events.

After proper format conversion of the RSC P and S arrival time dataset, we proceed to Step 2 and test the Rapid Earthquake Association and Location code - REAL (Zhang et al. 2019). The algorithm REAL associates phases to a seismic event using a grid-search method and a travel-time table. REAL initially counts the number of P and S picks and then calculates the travel-time residuals. Many constraints can be set to enhance association reliability based on station gap, outlier removal based on the variation of distance and/or travel-time residual, and the number of stations with both P and S picks, among others.

Examining the RSC catalog, we find that the minimum time between events is about 3 s and the minimum number of phases used to locate an event is 4, although only in one case. Based on this information, and to minimize the discrepancy between the number of events associated with REAL and those in the original catalog, we set a minimum threshold of 4 arrival times to declare an event with REAL, and also adjust the other parameters.

We use a uniform velocity model from Peruzza et al. 2022a ($V_p = 5.85$ km/s, and $V_p/V_s = 1.78$) and a 10 km search range centered on the station that recorded the earliest seismic phase, extended to a maximum depth of 20 km. The search grid was set to be approximately 2 km horizontally and in depth.

The chosen REAL parameter's configuration provides a number of earthquakes equal to 100% of the original RSC catalog, using the manual picks and, as a proxy for common events, a tolerance of 1.5 s in the origin time differences between the two catalogs. This large tolerance is appropriate at this stage since we are pairing the preliminary REAL earthquake locations with the refined manual ones. In our process, REAL's primary function is to associate proper picks, whereas absolute and relative locators enhance location accuracy in the following LOC-FLOW steps (3 and 4, respectively).

Some notes on the differences between the number of phases associated with the same event by REAL and the one reported in the RSC original catalog are worthwhile here. Most of the picks are consistently associated; in particular about 98% of the events have ± 1 phases difference, while 2% differ in 2 or more associated phases, up to a maximum difference of 4. In some cases, the REAL algorithm is unable to properly associate the correct picks combination due to travel-time residuals at certain stations that conflict with the imposed constraints. Therefore, minimum differences exist between a rigorous manual revision procedure (RSC catalog) and an unsupervised automatic association of the same picks.

The current test is ideal, since all the RSC picks are true ones, related to certified earthquakes. When using REAL on automatic picks (obtained by machine learning), a significant number of false picks are introduced, hopefully rejected by the associator.

The subsequent absolute earthquake location (Step 3) is applied using the results of REAL RSC phase association. We maintain the original RSC P and S picking weights (0-3) using Hypoellipse and utilize the same 1D velocity model and station residuals as Peruzza et al. (2022a). The velocity model was obtained using a genetic algorithm technique, as described in Romano et al. (2019). The station residuals are a combination of two components, i.e. the topographic and the unmodeled velocity structure: the first one is computed by Hypoellipse according to the station elevation and the velocity values associated to the crustal layer above the sea level ($V_p = 4.0$ km/s, and $V_p/V_s = 1.84$); the second one was computed based on the statistics of the residuals of Hypoellipse run with the option RELOCATE, for the first years of RSC monitoring (as in Romano et al. 2019). Figure 2a–c shows a comparison of the horizontal and vertical error and rms origin time, as obtained by Peruzza et al. (2022b) and in this study at this stage of processing, where the only significant difference between the two catalogs is related to the picks association procedure. The results are consistent, and the location differences are all centered around 0; therefore the differences related to the picking association procedure do not alter the spatial features that characterize the sequence.

After verifying the workflow performed up to this stage, we restart the procedure by activating the ML picker PhaseNet (second branch of Step 1 in Figure 1b), instead of using the RSC original manual picks. We apply PhaseNet on daily continuous seismic waveforms using the high-pass filtering (1 Hz) option for data preprocessing, which is recommended for microseismicity detection as it improves picking performance for events with very low signal-to-noise ratios. This setting can be changed for real-time applications when we do not know if the system will locate microseismicity or major events.

PhaseNet produces probability distributions for P-wave and S-wave arrivals, with the probability peak aligned to the corresponding phase arrival time. By default, the threshold probability for a potential pick is about 0.3, below this value, noisy signals prevail (Zhu and Beroza 2019). We obtain a total of 81645 P and 63560 S picks, of which 9046 and 4340 respectively, characterized by a probability value greater than 0.8 (Figure 3a and b). Using a low probability threshold (e.g. <0.5) inevitably introduces false picks, which could potentially reduce the accuracy of the location

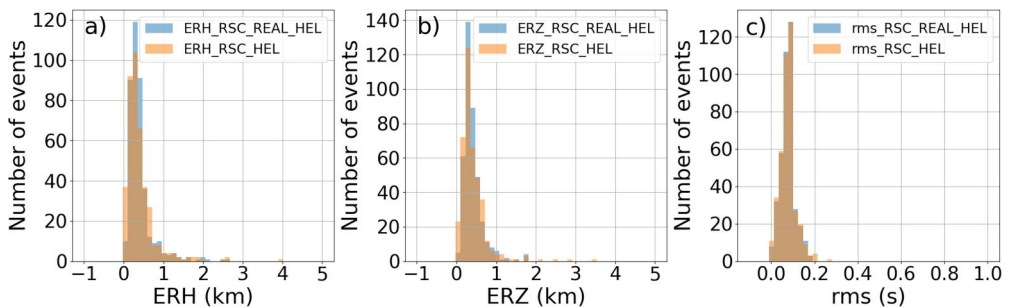


Figure 2. Absolute location analysis, obtained from steps 1–3 (see Figure 1b) with RSC manual picks. a) Comparison of the horizontal, b) vertical errors and c) rms of origin times for the Hypoellipse locations obtained by Peruzza et al. (2022b) and the ones obtained in this study using the manual RSC P and S picks, and the REAL associator (in orange and light blue respectively).

precision, but as previously said, we expect most false picks to be dismissed during the association phase since they are inconsistent across multiple stations.

In fact, false positive and false negative phase arrivals are always present in the ML output, the former are usually removed when associating phase picks over a seismic network, while the second may result in earthquakes being missed (e.g. Park et al. 2023).

Figure 3c and d shows the distribution of the time difference between PhaseNet and manual RSC picks at the same stations for P and S phases, using as a pairing rule a window of ± 0.5 s for common picks. At this stage, we are comparing only the performance of the ML picker. About 79% and 90% of the RSC picks are commonly detected for P and S, respectively. The majority of them show PhaseNet probability values greater than 0.8.

A non-negligible percentage of picks are missed (false negative, as previously stated) by the PhaseNet approach, particularly for P phases. Investigating the reason for this behavior, we find that in many cases PhaseNet is unable to recognize phases associated with almost overlapping events (Figure 3e), that are conversely identified by human analysis. In other cases, the ML picker does not perform well due to the low signal-to-noise ratio that characterizes low magnitude events. Nonetheless, PhaseNet identifies high probability P and S picks (>0.8) that are not listed in the manual catalog and that could be potentially associated with true events.

While P pick time differences at common stations are almost centered around zero, we observe a systematic delay for PhaseNet S picks (Figure 3d). This may be attributed to differences in the manual picking procedures used to train PhaseNet compared to those used in our study. The feature is particularly evident as the associated PhaseNet probability value decreases.

PhaseNet picks are then used as input to the REAL package to associate them into individual seismic events. We visually reviewed phase picks and their probabilities and determined that all with a probability 0.4 or less should be excluded to limit the presence of a large number of inconsistent picks at this stage of the processing. As a consequence, the percentage of common P and S picks shown in Figure 3c and d drop to 76% and 88% respectively ($-0.3/-0.2\%$).

We use almost the same configuration adopted for the association of RSC picks; however, when using REAL on ML picks, a significant number of false picks exist and some constraints have to be adopted to limit fake events. Therefore, we slightly increase the number of associated P and S phases, assuming that each event will have a minimum of 3 P picks, 1 S pick, and at least one station with both P and S picks. In general, including a minimum number of stations with both P and S picks is crucial to avoid regional earthquakes being interpreted as local ones during unsupervised processing.

Compared to the original catalog and using 1.5 s in origin time as a proxy for common events (just like before), 372 RSC events ($\sim 91\%$) are found, while 35 ($\sim 9\%$) are lost, and 192 new potential events are identified. The missing events have, on average, a number of associated P phases less than 10 in the RSC catalog. As for the new potential events, they are characterized, on average, by a number of phases less than 7, and a significant azimuthal gap ($>240^\circ$). Therefore, we could expect that a

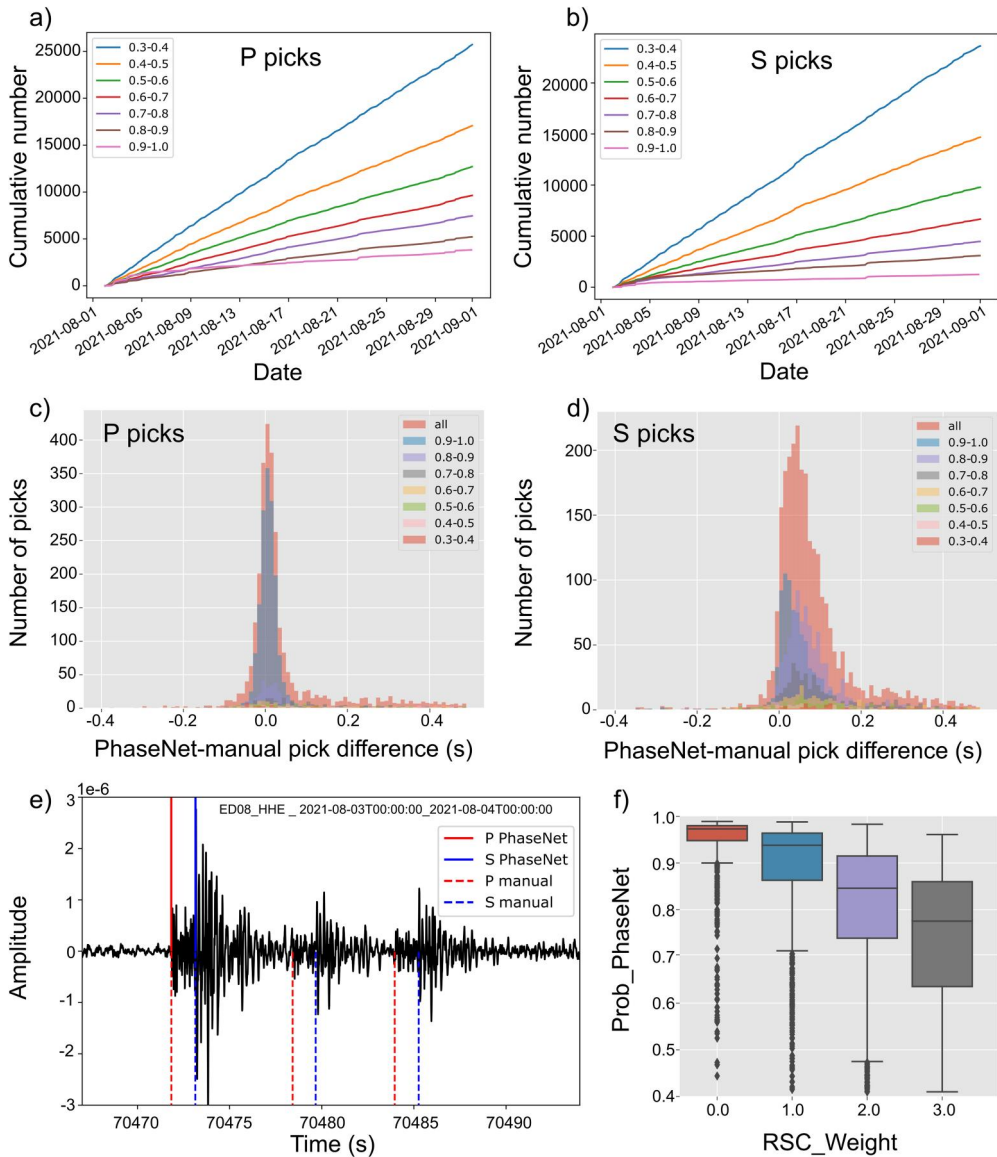


Table 1. Corresponding values used between manual time pick uncertainties, Hypoellipse weights and PhaseNet probabilities.

Pick uncertainty (sec)	Hypoellipse weight	PhaseNet probability					
0.00 – 0.02	0	1.00 – 0.95		1.00 – 0.95			
0.02 – 0.05	1	0.95 – 0.86		0.95 – 0.86			
0.05 – 0.12	2	0.86 – 0.74		0.86 – 0.74			
0.12 – 0.3	3	0.74 – 0.40		0.74 – 0.63			
n.d	4	<0.4		<0.63			
		Total events			Total events		
		464			421		
		RSC (407)	New	New	RSC	New	New
		Common	false	true	(407) Common	false	true
		<i>(1s origin time)</i>			<i>(1s origin time)</i>		
		363 (~89% RSC)	18	83	351 (~86% RSC)	2	68

We tested two different configurations for weight 3. One assuming the 1st quantile distribution (conservative), and another one including all the picking with a probability value bigger than 0.4, associated by REAL. For each configuration, the number of total events characterized by horizontal and vertical error less than 5 km, and gap <300° are shown. The number of common events with the RSC catalog is also shown (using as a proxy for common events 1 s in the origin time difference), together with a quantification of the new false and new true detected events respectively. Events are classified true or false after visual inspection of the associated seismic waveforms.

considerable part of them will be discarded in the subsequent absolute and relative location steps, with filters based on horizontal and vertical errors, and azimuthal gap.

To address Step 3, devoted to absolute location, before using the Hypoellipse module we have to convert the ML picking probability estimation provided by PhaseNet into Hypoellipse weights. The choice of weight assignment is critical since it significantly impacts the inversion process that minimizes residuals during the earthquake location procedure. The lower the phase weight code, the lower the uncertainty of the picking time (see Table 1) and the higher the importance attributed to this reading by the Hypoellipse code during the inversion process.

We calibrate the conversion by analyzing the distribution of PhaseNet pick probability and the pick's weight in the original catalog for common picks (tolerance to pair picks lowered to 0.3 s). Figure 3f shows that there is no unique, well-constrained correlation, and high probability values (e.g. 0.9) may also be associated with high Hypoellipse weights (e.g. 3), and vice versa. Nevertheless, a general trend can be defined if we consider the distribution of the useful dataset, estimated in the range from 0.4 to 1.0 PhaseNet probabilities. Table 1 shows the values used to correlate probabilities and weights, using as a proxy the 1st quartile (25%) distributions for RSC weights from 0 to 3. We also test a less conservative probability threshold for weight 3, including all the picks associated by REAL in the localization process and characterized by a probability value above 0.4. Based on the results shown in Table 1, we decide to select the correlation strategy based on quartile values that yields the lowest number of false events.

In the end, a final catalog with 421 events is obtained, with 351 events in common with the original RSC manual catalog (~86% of the RSC catalog is reached), if we use a 1 s tolerance window for origin time, and excluding the events with horizontal and vertical error >5 km, and azimuthal gap >300°.

With these quality constraints, about 5% of RSC events are missed, compared to the REAL output percentage previously observed (from 91% to 86%), but we are

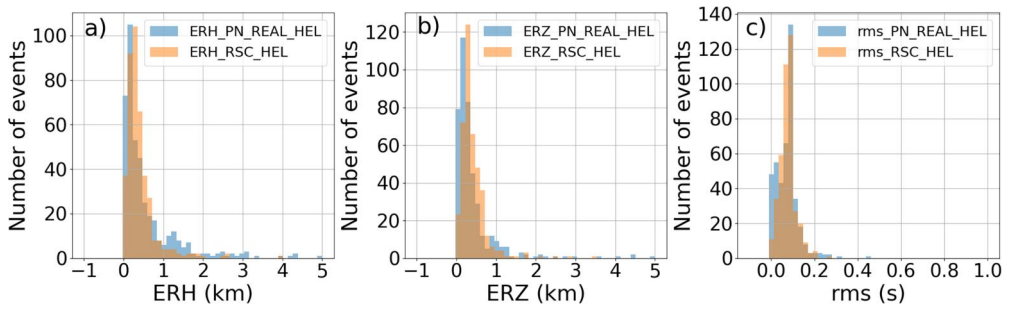


Figure 4. Absolute location analysis, obtained from steps 1 to 3 (see [Figure 1b](#)) with PhaseNet picks. a) Comparison of the horizontal, b) vertical errors and c) rms origin times for the Hypoellipse locations obtained by Peruzza et al. (2022b) and the ones obtained in this study using the PhaseNet P and S picks and REAL as associator (in orange and light blue respectively). See [Figure 2](#) for comparison with the RSC manual picks.

fairly confident about the quality of the dataset, since a negligible number of false events is introduced ([Table 1](#)).

The LOC-FLOW code performs well also for the events outside the Refrontolo area, highlighting the sequence that occurred in the Alpage area during the same period. In fact, out of the 421 found events, 41 are characterized by latitude greater than 46° N (see the dataset in [Figure 1a](#)), and only some events are located westward (longitude lower than 12° E).

[Figure 4a–c](#) compares some features of the Refrontolo sequence, whose absolute hypocenters were fully checked by manual controls in Peruzza et al. (2022a), with the ones obtained automatically, using PhaseNet ML picks (weights are assigned as described above) and REAL associator. The new catalog shows higher values for horizontal errors for some events, but the general trend is rather similar.

Then, relative locations (Step 4 in [Figure 1b](#)) are determined using HypoDD (Waldhauser and Ellsworth 2000) with the conjugate gradients method (LSQR), since the singular value decomposition (SVD) is only applicable to a limited number of events. We make only minor adjustments to the code to ensure proper weighting in the input format of the HypoDD phase time file, which matches the Hypoellipse weighting for differential travel time. We use both time and cross-correlation modules, and we complete the HypoDD_dtct procedure before starting HypoDD_dtcc one; in fact to have accurate initial locations for dt.cc we use dt.ct locations to update the phase file as a strategy.

The HypoDD weights in the cross-correlation mode are estimated based on cross-correlation values in the frequency band of 5–15 Hz, using a minimum correlation coefficient of 0.6. This frequency band was chosen because of the low magnitude of the events and the associated corner frequency estimated in Peruzza et al. (2022a). Starting from 421 events, we relocated 341 events with HypoDD.

The final absolute and relative locations of the Refrontolo seismic sequence are shown in [Figure 5](#), and compared with those of the RSC. The earthquakes' cloud defined automatically is elongated further south than before, probably an effect of the shift for the S phases picking. For the relative locations, the activated structure

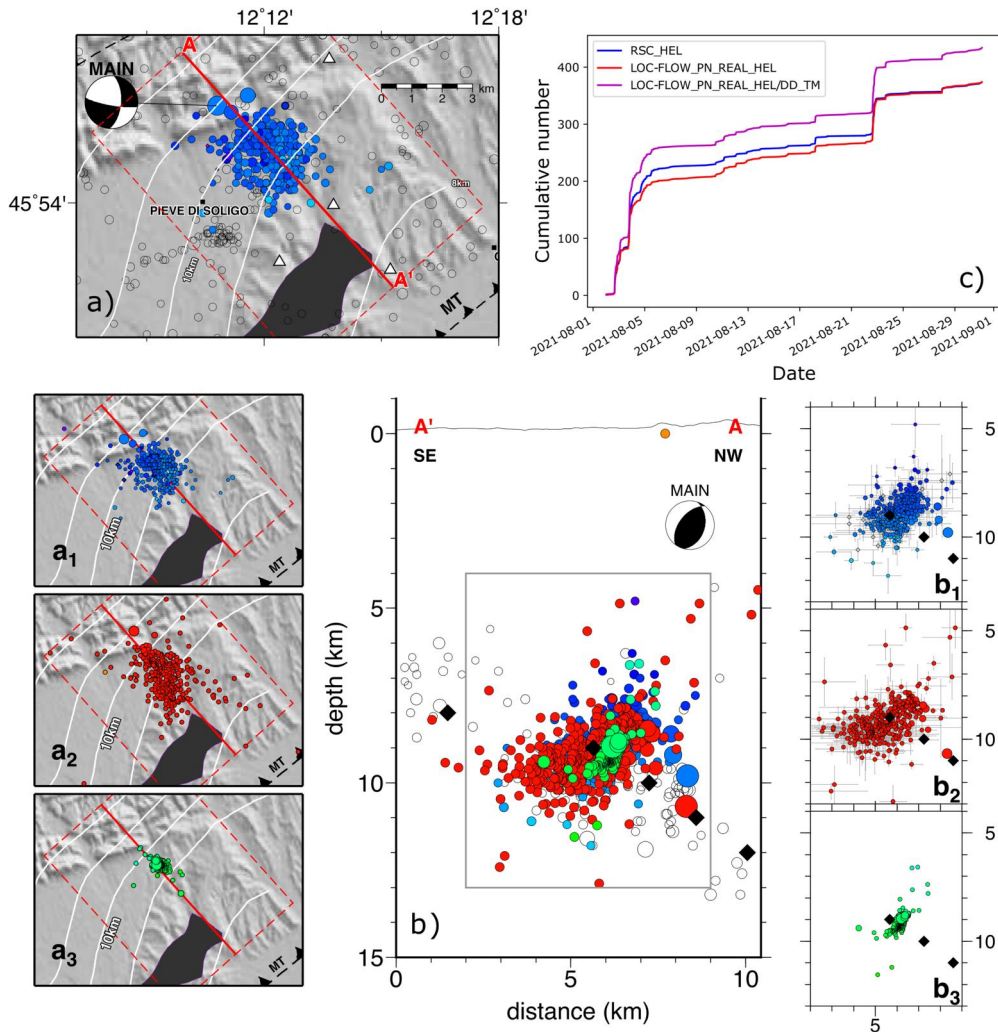


Figure 5. Manual versus automatic locations for the Refrontolo sequence. Panels a) epicentral maps of the original Hypoellipse dataset provided in Peruzza et al. (2022a) in a₁), transparent circles show the location of the seismicity detected from 2012 in the region; a₂) dataset obtained with ML phase picker PhaseNet, REAL and Hypoellipse; a₃) dataset of the LOC-FLOW relative location with HypoDD cross-correlation obtained with ML phase picker PhaseNet, REAL and Hypoellipse. Panels b) cross sections of the same subsets as before, overlapped, respectively in b₁) absolute location; b₂) relative location as in a₃. The trace of the vertical section is plotted in red, the Montello thrust represented by isobaths (white curve lines) is taken from Picotti et al. (2022). The intersections of the isobaths with the plane of the vertical section are marked by black rhombs. Panel c) comparison of the cumulative number of events over time for the Refrontolo sequence (only events of the Refrontolo sequence are considered - inside the green box of Figure 1a), original RSC Hypoellipse dataset provided in Peruzza et al. (2022a) (blue), Hypoellipse LOC-FLOW catalog using the PhaseNet P and S picks and REAL as associator (red), and template matching LOC-FLOW catalog using the PhaseNet P and S picks, REAL and Hypoellipse/HypoDD as input catalog (magenta).

appears as an antithetic feature to the main Montello thrust depicted by the previous seismicity (black open circles, and black diamonds, in [Figure 5b](#)) with an inclination perfectly consistent with the one resulting from the focal mechanism of the main event of the sequence.

Finally, we also test the template matching module, using the approach included in the LOC-FLOW procedure ([Zhang and Wen 2015](#)), for the events of the Refrontolo sequence only. This reduced the number of usable templates from 421 to 374.

Template matching has been used to improve seismic catalogs since 2006 ([Gibbons and Ringdal 2006](#); [Shelly et al. 2007](#)), increasing the capability to recognize and analyze spatio-temporal seismic patterns that characterize seismic sequences both in well-instrumented (e.g. [Kato et al. 2012](#); [Vuan et al. 2020](#); [Sugan et al. 2023](#); [Sugan et al. 2019](#)) and remote regions ([Cesca et al. 2022](#)). Starting from well-located events, continuous seismic data are scanned to search for possible similar events. We use the absolute/relative location (output of Step 3 and 4, performed with PhaseNet pickings, REAL associations and Hypoellipse/HypoDD locations) as templates in our procedure, using 3 s window length waveforms and the RSC stations only, limiting the analysis to the events located in the Refrontolo region. The signal was filtered using a 5-15 Hz bandpass. The code computes the mean correlation coefficient (CC) value and Median Absolute Deviation (MAD) of the stacked cross-correlograms. When the mean CC and MAD values exceed the defined thresholds, a positive detection is declared, assuming the same location of the event with the maximum mean CC value.

We select as positive detections all the events with $CC > 0.65$ and $MAD > 15$. This last step allows increasing the number of events in the catalog ([Figure 5c](#)) for the Refrontolo sequence. Starting from 374 templates, we found 60 newly detected events. Comparing the new extended catalog (434 events) with the corresponding RSC subset (374 events in the region delimited by the green box in [Figure 1a](#)) and using as a proxy 1 sec in the origin travel time differences, we found that $\sim 93\%$ of the RSC events are in common.

The cumulative number of events over time shows that the template matching recovers the seismicity missed during the most productive days of the sequence (August 2 and 3), enhancing the number of detected events with respect to RSC during this period. This is not surprising, since the technique itself is able to recognize seismic signals hidden in the noise or masked by overlapping events, where P and S picks cannot be manually set.

3. Discussion

The use of new ML algorithms to analyze large seismic datasets is critical for monitoring the temporal evolution of seismicity in a complex geological system and for understanding the physical processes involved in generating moderate to large earthquakes that may be anticipated by the occurrence of small seismic events.

ML pickers have great potential for the analysis of microseismicity, but they still need to be used with attention. In this study, we applied a machine-learning based approach on a microearthquake seismic sequence, with local magnitudes in the range

from -0.6 to 2.5 . We obtained about 21% less P-wave picks than with manual phase picking. This is understandable for quasi-overlapping events, where the coda of the preceding event masks the P onset of the following event; the performance of neural phase pickers also seems related to the low signal to noise ratio of the microevents. Similar to Kim et al. (2023), we emphasize the need to train the ML algorithm including overlapping events into the training data to improve the detection performance when many earthquakes occur in a short period of time. This will require supervised training methods where a dataset of manual phase picks have been made for overlapping events. In other situations the false negative P phase could be related to picks prediction inconsistency. Concerning prediction inconsistency, Park et al. (2023) showed that the probability associated with the ML picks can change with even a small perturbation of the input waveform. They also highlighted that a high value in the picking classification probability does not necessarily imply a reliable phase pick. While developers consider these observations to improve neural phase pickers, other inputs may come from end users comparing the results of ML picks to an overall location process that uses well-suited seismic sequences as a benchmark, as done in this study.

Analysis of PhaseNet probabilities also shows that probability values vary compared to pick uncertainties determined by manual revision. Nevertheless, a general trend can be identified, and appropriate conversion should be made between PhaseNet probabilities, temporal pick uncertainties, and Hypoellipse weights.

In our study, the automatic S picks provided by PhaseNet (Figure 3d) are generally delayed compared to the manual S picks. S-arrival times can be difficult to detect, especially when the complexity of the structure over which the waves propagate can lead to P-S conversion. It is not possible to distinguish converted phases from PhaseNet results. Since the manual RSC S-picks were scrupulously reviewed, we assume that such features are likely to be found in other case studies. This aspect should be kept in mind by developers and end users when testing different ML pickers and models or improving existing ones.

Despite the differences in picking, Figure 5 shows that the seismicity obtained in a fully automatic way, with PhaseNet ML picks in the LOC-FLOW procedure, reconstructs well the geometry of the activated fault, depicted by the manual processing in Peruzza et al. (2022a), in agreement with the focal mechanism obtained from the polarity for the strongest event of the sequence. These findings enrich the observations on the active tectonic structure that characterizes the studied area (Restivo et al. 2016; Saraò et al. 2021).

LOC-FLOW has also proved useful in correctly identifying and locating events in the periphery of the study region, in the Alpage area. Of the total 421 Hypoellipse events, 31 belong to the Alpage sequence located in the northern part of the region (between 46° and 46.2° latitude), while other 16 events are located at a greater distance from the Refrontolo sequence (outside the region delimited by the green box in Figure 1a).

Our results show that with the ML picks alone up to the absolute location step, $\sim 86\%$ of the events in the RSC catalog are found using as a proxy 1 s time difference in the origin time and quality constraints based on the horizontal and vertical errors and associated weights, as shown in Table 1.

Finally, we test the template matching module; it increases the number of events detected with respect to the manually located ones (Figure 5c): this is particularly evident during the most productive period of the Refrontolo sequence (August 2-3, 2021, Figure 1a₃). Nevertheless, a maximum of ~93% RSC events are found, not reaching 100%, using the selected thresholds. This means that a minimum percentage of the RSC events are not found by the new procedure, and vice versa.

Despite the promising results we have obtained with LOC-FLOW, some issues need to be considered before applying the methodology, especially with regard to the purpose of the output catalog.

Spurious picks and associated unsupervised events do not seem to affect the main spatio-temporal features of the sequence (Figure 5.), but the systematic delay observed for S-picks leads to a systematic shift in the observed event cloud which is partially compensated by relative location.

Therefore, manual robust revision is still required for some specific applications. This is particularly true for all activities related to monitoring of induced seismic events, for which high quality certified data must be provided and which may have legal implications. At the same time, in the case of productive sequences, ML-based detection may be an optimal strategy to quickly generate earthquake catalogs that are reliable enough to make decisions for seismic risk mitigation.

So far, we encourage developers to improve ML methods, emphasizing the need to train models on massive, very local data as they become available, and also to consider and address the aspect of picking inconsistency as pointed out by Park et al. 2023.

For further research, we plan to test different configurations of ML pickers, including PhaseNet, trained on different datasets (Münchmeyer et al. 2022) in the hope of improving the results obtained.

4. Conclusion

In this study, we test the performance of the machine learning PhaseNet technique integrated into the LOC-FLOW code for detecting microseismicity in the Montello region, in northeast Italy. Seismic monitoring of the region is extremely important due to the Collalto gas reservoir that has been in operation since 1994 and instrumentally monitored by RCS since 2012; so far, all the seismic activity has been considered of natural origin. We use an unusually productive microseismic sequence that occurred near Refrontolo in August 2021 as a case study.

Our results show that PhaseNet detected 79% and 90% of the manual P and S arrival times at the same stations, respectively, using a 0.3 probability threshold and the model trained on the original California dataset. While P picks show enough accuracy, we observe a general delay for the S picks, which we expect should be a common feature even in other datasets, based on the high quality of the manual picking used for comparison.

If we include the events detected by the template matching procedure, the final LOC-FLOW catalog has an increased number of events compared with the initial manual one. Nonetheless, in our case study, PhaseNet does not help increase the

earthquake number during the most productive days of the sequence (e.g. 2-3 August), and template matching is crucial during these intervals. We acknowledge that there are several tuning steps in the LOC-FLOW package, and each choice of parameters plays a role in the resulting number of events identified. Despite the lower accuracy in S picks, PhaseNet performances are good, especially if we consider that the automatic procedures require much less working time in comparison with the manual picking. The observed seismicity clearly depicted the geometry of the activated fault in both time and space. Our results show that LOC-FLOW can effectively and accurately produce earthquake catalogs by processing continuous seismic data, and that it can effectively support very dense local networks during seismic monitoring even for very low-magnitude events.

At the same time, we acknowledge that ML techniques may not yet be ready to replace the standard approach in compiling certified seismic catalogs for microseismic sequences. Some limitations may depend on the original training used. We plan to test different ML picker configurations trained on different dataset, hopefully increasing the obtained results. In this study, we show that the integration of template matching code is important to recover missed events and increase the number of events. We would encourage the use of ML at a very local scale, where a preliminary comparison with benchmark data manually processed for the area under investigation should be considered.

Acknowledgments

This work is done in the frame of the activities that OGS performs for seismic monitoring of industrial sites. The Collalto Seismic Network is managed by OGS on behalf of Edison Stoccaggio S.p.A. in compliance with the requirements of the Italian Ministry of Environment, Land and Marine Protection (MATTM) and in agreement with the Veneto Region. The authors would like to thank Enrico Priolo and the technical and control room staff: Fabio Franceschinell, Marco Santulin, Paolo Bernardi, Peter Klin, Giovanna Laurenzano, Franco Pettenati, Alessandro Rebez, and Angela Saraò.

Author contributions

MS performed conceptualization, data analyses, and representation, original draft and manuscript handling. LP performed data representation. LP, MAR, MG, LM, DS, MPPL and MR contributed to data interpretation, manuscript writing, reviewing and editing.

Disclosure statement





No potential conflict of interest was reported by the authors.

Funding

This study was carried out in the frame of the Italian PRIN Project 'Fault segmentation and seismotectonics of active thrust systems: the Northern Apennines and Southern Alps laboratories for new Seismic Hazard Assessments in northern Italy (NASA4SHA)' (PI R. Caputo, UR Responsible L. Peruzza). The research was also supported by OGS and CINECA under HPC-TRES program.

This paper does not represent OGS, or gas storage concession holders, official opinion and policies.

ORCID

Monica Sugan  <http://orcid.org/0000-0002-1247-3193>
 Laura Peruzza  <http://orcid.org/0000-0001-7781-5775>
 Maria Adelaide Romano  <http://orcid.org/0000-0002-7191-0496>
 Mariangela Guidarelli  <http://orcid.org/0000-0003-0481-9366>
 Luca Moratto  <http://orcid.org/0000-0001-6328-2138>
 Denis Sandron  <http://orcid.org/0000-0002-1143-9954>
 Milton Percy Plasencia Linares  <http://orcid.org/0000-0002-6218-8411>
 Marco Romanelli  <http://orcid.org/0000-0002-7360-0459>

Data availability statement

The data cited and used in this study (Peruzza et al. 2022b) are available in Zenodo Open Access repository, <https://doi.org/10.5281/zenodo.7252308>.

The continuous data of the RSC seismic network, and of the SMINO Network are available from OASIS Web Services (Priolo et al. 2015b), <http://oasis.crs.inogs.it>.

The following codes are available on github, PhaseNet: <https://github.com/wayneweiqiang/PhaseNet>; REAL: <https://github.com/Dal-mzhang/REAL>; FDTCC: <https://github.com/MinLiu19/FDTCC>; Match&Locate: <https://github.com/Dal-mzhang/MatchLocate2>; LOC-FLOW: <https://github.com/Dal-mzhang/LOC-FLOW>, last access April 2023. hypoDD software available at <https://www.ldeo.columbia.edu/~felixw/hypoDD.html>; Hypoellipse software available at <https://pubs.usgs.gov/of/1999/ofr-99-0023/>.

References

- Anikiev D, Birnie C, bin Waheed U, Alkhalifah T, Gu C, Verschuur DJ, Eisner L. 2023. Machine learning in microseismic monitoring. *Earth Sci Rev.* 239:104371. doi:10.1016/j.ear-scirev.2023.104371.
- Bragato PL, Comelli P, Saraò A, Zuliani D, Moratto L, Poggi V, Rossi G, Scaini C, Sugan M, Barnaba C, et al. 2021. The OGS–Northeastern Italy seismic and deformation network: current status and outlook. *Seismol Res Lett.* 92(3):1704–1716. doi:10.1785/0220200372.
- Bragato PL, Di Bartolomeo P, Pesaresi D, Plasencia Linares MP, Saraò A. 2011. Acquiring, archiving, analyzing and exchanging seismic data in real time at the Seismological Research Center of the OGS in Italy. *Ann Geophys.* 54(1):67–75. doi:10.4401/ag-4958.
- Burrato P, Poli ME, Vannoli P, Zanferrari A, Basili R, Galadini F. 2008. Sources of Mw 5+ earthquakes in northeastern Italy and Western Slovenia: an updated view based on geological and seismological evidence. *Tectonophysics.* 453(1–4):157–176. doi:10.1016/j.tecto.2007.07.009.
- Cesca S, Sugan M, Rudzinski L, Vajedian S, Niemz P, Plank S, Petersen G, Deng Z, Rivalta E, Vuan A, et al. 2022. Massive earthquake swarm driven by magmatic intrusion at the Bransfield Strait, Antarctica. *Commun Earth Environ.* 3(1):89. doi:10.1038/s43247-022-00418-5.
- Galadini F, Poli ME, Zanferrari A. 2005. Seismogenic sources potentially responsible for earthquakes with $M \geq 6$ in the eastern Southern Alps (Thiene-Udine sector, NE Italy). *Geophys J Int.* 161(3):739–762. doi:10.1111/j.1365-246X.2005.02571.x.
- Garbin M, Priolo E. 2013. Seismic event recognition in the Trentino area (Italy): performance analysis of a new semiautomatic system. *Seismol Res Lett.* 84(1):65–74. doi:10.1785/0220120025.

- Gibbons SJ, Ringdal F. 2006. The detection of low magnitude seismic events using array-based waveform correlation. *Geophys J Int.* 165(1):149–166. doi:[10.1111/j.1365-246X.2006.02865.x](https://doi.org/10.1111/j.1365-246X.2006.02865.x).
- Kato A, Obara K, Igarashi T, Tsuruoka H, Nakagawa S, Hirata N. 2012. Propagation of slow slip leading up to the 2011 M_w 9.0 Tohoku-Oki earthquake. *Science.* 335(6069):705–708. doi:[10.1126/science.1215141](https://doi.org/10.1126/science.1215141).
- Kim A, Nakamura Y, Yukutake Y, Uematsu H, Abe Y. 2023. Development of a high-performance seismic phase picker using deep learning in the Hakone volcanic area. *Earth Planets Space.* 75(1):85. doi:[10.1186/s40623-023-01840-5](https://doi.org/10.1186/s40623-023-01840-5).
- Kong Q, Trugman DT, Ross ZE, Bianco MJ, Meade BJ, Gerstoft P. 2019. Machine learning in seismology: turning data into insights. *Seismol Res Lett.* 90(1):3–14. doi:[10.1785/0220180259](https://doi.org/10.1785/0220180259).
- Lahr JC. 1999. HYPOELLIPSE: a computer program for determining local earthquake hypocentral parameters, magnitude and first motion pattern (Y2K compliant version), US Department of the Interior, US Geological Survey: Reston, VA. Open-File Rep. 99–23, version 1.1, 119 p.
- Moratto L, Romano MA, Laurenzano G, Colombelli S, Priolo E, Zollo A, Saraò A, Picozzi M. 2019. Source parameters analysis of microearthquakes recorded around the underground gas storage in the Montello-Collalto Area (Southeastern Alps, Italy). *Tectonophysics.* 762:159–168. doi:[10.1016/j.tecto.2019.04.030](https://doi.org/10.1016/j.tecto.2019.04.030).
- Moratto L, Sandron D. 2015. Optimizing the automatic location of the real-time Antelope system in north-eastern Italy. *Boll Geof Teor Appl.* 56:407–424. doi:[10.4430/bgta0154](https://doi.org/10.4430/bgta0154).
- Mousavi SM, Horton SP, Langston CA, Samei B. 2016. Seismic features and automatic discrimination of deep and shallow induced-microearthquakes using neural network and logistic regression. *Geophys J Int.* 207(1):29–46. doi:[10.1093/gji/ggw258](https://doi.org/10.1093/gji/ggw258).
- Mousavi SM, Zhu W, Sheng Y, Beroza GC. 2019. CRED: a deep residual network of convolutional and recurrent units for earthquake signal detection. *Sci Rep.* 9(1):10267. doi:[10.1038/s41598-019-45748-1](https://doi.org/10.1038/s41598-019-45748-1).
- Münchmeyer J, Woollam J, Rietbrock A, Tilmann F, Lange D, Bornstein T, Diehl T, Giunchi C, Haslinger F, Jozinović D, et al. 2022. Which picker fits my data? A quantitative evaluation of deep learning based seismic pickers. *JGR Solid Earth.* 127(1):e2021JB023499. doi:[10.1029/2021JB023499](https://doi.org/10.1029/2021JB023499).
- NCEDC. 2014. Northern California earthquake data center. UC Berkeley Seismological Laboratory. Dataset. doi:[10.7932/NCEDC](https://doi.org/10.7932/NCEDC).
- Panebianco S, Serlenga V, Satriano C, Cavalcante F, Stabile TA. 2023. Semi-automated template matching and machine-learning based analysis of the August 2020 Castelsaraceno microearthquake sequence (southern Italy). *Geomatics Nat Hazards Risk.* 14(1). doi:[10.1080/19475705.2023.2207715](https://doi.org/10.1080/19475705.2023.2207715).
- Park Y, Beroza GC, Ellsworth WL. 2023. A mitigation strategy for the prediction inconsistency of neural phase pickers. *Seismol Res Lett.* 94(3):1603–1612. doi:[10.1785/0220230003](https://doi.org/10.1785/0220230003).
- Peruzza L, Romano MA, Guidarelli M, Moratto L, Garbin M, Priolo E. 2022a. An unusually productive microearthquake sequence brings new insights to the buried active thrust system of Montello (Southeastern Alps, Northern Italy). *Front Earth Sci.* 10:1044296. doi:[10.3389/feart.2022.1044296](https://doi.org/10.3389/feart.2022.1044296).
- Peruzza L, Romano MA, Guidarelli M, Moratto L, Garbin M, Priolo E. 2022b. Microearthquake sequence recorded close to the Montello thrust system (Southeastern Alps) [Data set]. Zenodo. doi:[10.5281/zenodo.7252308](https://doi.org/10.5281/zenodo.7252308).
- Picotti V, Romano MA, Ponza A, Guido FL, Peruzza L. 2022. The Montello thrust and the active mountain front of the eastern Southern Alps (northeast Italy). *Tectonics.* 41(12):e2022TC007522. doi:[10.1029/2022TC007522](https://doi.org/10.1029/2022TC007522).
- Priolo E, Laurenzano G, Barnaba C, Bernardi P, Moratto L, Spinelli A. 2015b. OASIS - the OGS archive system of instrumental seismology. *Seismol Res Lett.* 86(3):978–984. doi:[10.1785/0220140175](https://doi.org/10.1785/0220140175).
- Priolo E, Romanelli M, Plasencia Linares MP, Garbin M, Peruzza L, Romano MA, Marotta P, Bernardi P, Moratto L, Zuliani D, et al. 2015a. Seismic monitoring of an underground

- natural gas storage facility: the Collalto Seismic Network. *Seismol Res Lett.* 86(1):109–123. doi:[10.1785/0220140087](https://doi.org/10.1785/0220140087).
- Restivo A, Bressan G, Sugan M. 2016. Stress and strain patterns in the Venetian Prealps (north-eastern Italy) based on focal-mechanism solutions. *Boll Geofis Teor App.* 57(1):13–30. doi:[10.4430/bgta0166](https://doi.org/10.4430/bgta0166).
- Romano MA, Peruzza L, Garbin M, Priolo E, Picotti V. 2019. Microseismic portrait of the Montello thrust (southeastern Alps, Italy) from a dense high-quality seismic network. *Seismol Res Lett.* 90(4):1502–1517. doi:[10.1785/0220180387](https://doi.org/10.1785/0220180387).
- Ross ZE, Meier MA, Hauksson E, Heaton TH. 2018. Generalized seismic phase detection with deep learning. *Bull. Seismol. Soc. Am.* 108(5A):2894–2901. doi:[10.1785/0120180080](https://doi.org/10.1785/0120180080).
- Saraò A, Sugan M, Bressan G, Renner G, Restivo A. 2021. A focal mechanism catalogue of earthquakes that occurred in the southeastern Alps and surrounding areas from 1928–2019. *Earth Syst Sci Data.* 13(5):2245–2258. doi:[10.5194/essd-13-2245-2021](https://doi.org/10.5194/essd-13-2245-2021).
- Scotto di Uccio F, Scala A, Festa G, Picozzi M, Beroza GC. 2023. Comparing and integrating artificial intelligence and similarity search detection techniques: application to seismic sequences in Southern Italy. *Geophys J Int.* 233(2):861–874. doi:[10.1093/gji/ggac487](https://doi.org/10.1093/gji/ggac487).
- Shelly DR, Beroza GC, Ide S. 2007. Non-volcanic tremor and low-frequency earthquake swarms. *Nature.* 446(7133):305–307. doi:[10.1038/nature05666](https://doi.org/10.1038/nature05666).
- Soto H, Schurr B. 2021. DeepPhasePick: a method for detecting and picking seismic phases from local earthquakes based on highly optimized convolutional and recurrent deep neural networks. *Geophys J Int.* 227(2):1268–1294. doi:[10.1093/gji/ggab266](https://doi.org/10.1093/gji/ggab266).
- Sugan M, Campanella S, Chiaraluce L, Michele M, Vuan A. 2023. The unlocking process leading to the 2016 Central Italy seismic sequence. *Geophys Res Lett.* 50(5):e2022GL101838. doi:[10.1029/2022GL101838](https://doi.org/10.1029/2022GL101838).
- Sugan M, Peruzza L. 2011. Distretti sismici del Veneto. *Boll Geofis Teor App.* 52:s3–s90. doi:[10.4430/bgta0057](https://doi.org/10.4430/bgta0057).
- Sugan M, Vuan A, Kato A, Massa M, Amati G. 2019. Seismic evidence of an early afterslip during the 2012 sequence in Emilia (Italy). *Geophys Res Lett.* 46(2):625–635. doi:[10.1029/2018GL079617](https://doi.org/10.1029/2018GL079617).
- Vuan A, Brondi P, Sugan M, Chiaraluce L, Di Stefano R, Michele M. 2020. Intermittent slip along the Alto Tiberina low-angle normal fault in central Italy. *Geophys Res Lett.* 47(17):e2020GL089039. doi:[10.1029/2020GL089039](https://doi.org/10.1029/2020GL089039).
- Waldhauser F, Ellsworth WL. 2000. A double-difference earthquake location algorithm: method and application to the northern Hayward fault, California. *Bull Seismol Soc Am.* 90(6):1353–1368. doi:[10.1785/0120000006](https://doi.org/10.1785/0120000006).
- Zhang M, Ellsworth WL, Beroza GC. 2019. Rapid earthquake association and location. *Seismol Res Lett.* 90(6):2276–2284. doi:[10.1785/0220190052](https://doi.org/10.1785/0220190052).
- Zhang M, Liu M, Feng T, Wang R, Zhu W. 2022. LOC-FLOW: an end-to-end machine-learning-based high-precision earthquake location workflow. *Seismol Res Lett.* 93(5):2426–2438. doi:[10.1785/0220220019](https://doi.org/10.1785/0220220019).
- Zhang M, Wen L. 2015. An effective method for small event detection: match and locate (M&L). *Geophys J Int.* 200(3):1523–1537. doi:[10.1093/gji/ggu466](https://doi.org/10.1093/gji/ggu466).
- Zhu W, Beroza GC. 2019. PhaseNet: a deep-neural-network based seismic arrival-time picking method. *Geophys J Int.* 216(1):261–273. doi:[10.1093/gji/ggy423](https://doi.org/10.1093/gji/ggy423).